



Identification of the dimethylamine-trimethylamine complex in the gas phase

Lin Du, Joseph R. Lane, and Henrik G. Kjaergaard

Citation: *J. Chem. Phys.* **136**, 184305 (2012); doi: 10.1063/1.4707707

View online: <http://dx.doi.org/10.1063/1.4707707>

View Table of Contents: <http://jcp.aip.org/resource/1/JCPSA6/v136/i18>

Published by the [American Institute of Physics](http://www.aip.org).

Additional information on *J. Chem. Phys.*

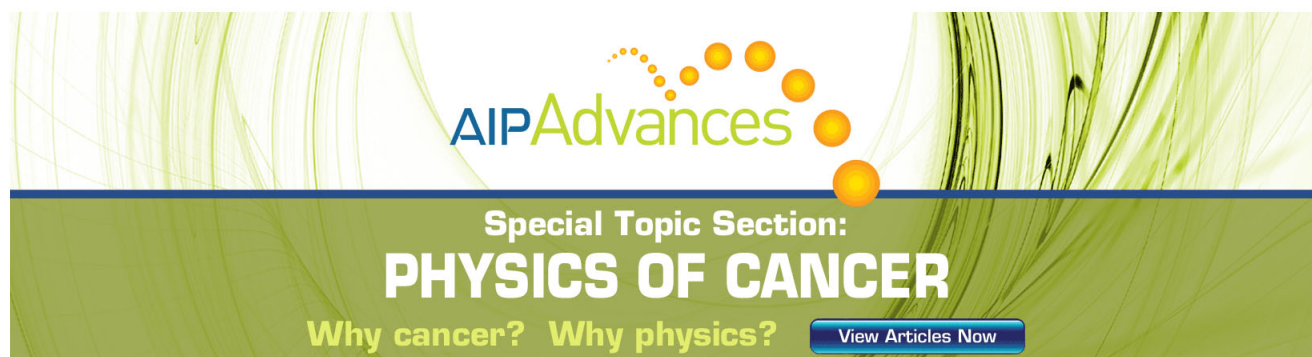
Journal Homepage: <http://jcp.aip.org/>

Journal Information: http://jcp.aip.org/about/about_the_journal

Top downloads: http://jcp.aip.org/features/most_downloaded

Information for Authors: <http://jcp.aip.org/authors>

ADVERTISEMENT



AIPAdvances

Special Topic Section:
PHYSICS OF CANCER

Why cancer? Why physics? [View Articles Now](#)

Identification of the dimethylamine-trimethylamine complex in the gas phase

Lin Du,¹ Joseph R. Lane,² and Henrik G. Kjaergaard^{1,a)}

¹Department of Chemistry, University of Copenhagen, Universitetsparken 5, DK-2100 Copenhagen Ø, Denmark

²Department of Chemistry, University of Waikato, Private Bag 3105, Hamilton 3240, New Zealand

(Received 13 February 2012; accepted 11 April 2012; published online 10 May 2012)

We have identified the dimethylamine-trimethylamine complex (DMA-TMA) at room temperature in the gas phase. The Fourier transform infrared (FTIR) spectrum of DMA-TMA in the NH-stretching fundamental region was obtained by spectral subtraction of spectra of each monomer. Explicitly correlated coupled cluster calculations were used to determine the minimum energy structure and interaction energy of DMA-TMA. Frequencies and intensities of NH-stretching transitions were also calculated at this level of theory with an anharmonic oscillator local mode model. The fundamental NH-stretching intensity in DMA-TMA is calculated to be approximately 700 times larger than that of the DMA monomer. The measured and calculated intensity is used to determine a room temperature equilibrium constant of DMA-TMA of $1.7 \times 10^{-3} \text{ atm}^{-1}$ at 298 K. © 2012 American Institute of Physics. [<http://dx.doi.org/10.1063/1.4707707>]

I. INTRODUCTION

Hydrogen bonded complexes in the Earth's atmosphere, especially hydrated complexes, have been investigated intensively.^{1–8} These weakly bound complexes are often studied experimentally under some form of cooling to favor complex formation. Due to the relatively low vapor pressures of the constituent molecules and the typically small equilibrium constants for complexation, it is difficult to study them under conditions relevant to the atmosphere. One feasible method is room temperature gas phase vibrational spectroscopy where frequency shifts of the XH (X = C,N,O) bond involved in the hydrogen bonding are observed.^{9–11}

Amines are good hydrogen bond acceptors and examples of recent Fourier transform infrared (FTIR) studies include: $\text{CHCl}_3\text{-NH}_3$,^{12,13} $\text{CH}_3\text{OH-TMA}$,¹⁴ and dimethylamine dimer (DMA-DMA).⁹ In these complexes, the XH bonds are elongated compared to bond lengths in the corresponding monomers. The associated hydrogen bonded XH-stretching fundamental transitions shift to lower wavenumbers (red shift)^{9,12–14} with an associated remarkable increase in the corresponding fundamental intensity. This increase in the fundamental IR intensity is often considered to be a defining feature of a conventional hydrogen bond.^{15,16}

A variety of methods have been used in experimental studies of hydrogen bonded complexes between amines to prove their existence.^{9,17–22} Lambert and Strong measured the compressibilities of ammonia and amines vapors to study dimer formation at temperatures between 20 and 130 °C.¹⁷ Pradeep *et al.* used ultraviolet photoelectron spectroscopy to detect the hydrogen bonded dimer of dimethylamine (DMA) in the vapor phase.¹⁸ Molecular beam studies by Odutola *et al.*¹⁹ of the electric deflection behaviors and polarity of

DMA dimer suggested a near linear hydrogen bond and the structure was determined by Fourier transform microwave rotational spectra.²⁰ Infrared photodissociation spectra of size selected methylamine (MMA) clusters were measured by Buck *et al.*²² FTIR spectra of 1:1 complexes of NH_3 with MMA, DMA, and trimethylamine (TMA) were measured in solid argon matrix.²¹ Recently, we measured the DMA dimer spectra with FTIR at room temperature.⁹ Association between DMA and TMA is expected to be similar to that in the DMA dimer and be dominated by an $\text{NH}\cdots\text{N}$ intermolecular hydrogen bond, since DMA is known to be a weak H-bond donor with a partial positive charge on H, and TMA is a strong H-bond acceptor with a partial negative charge on N atom.²³ Therefore, the DMA-TMA complex is a good example where the effects of hydrogen bonding on NH-stretching transitions can be investigated.

High level quantum chemical calculations not only guide experiments and help with interpretation of the experimental spectra, but also give reliable and accurate additional information on hydrogen bonding. The coupled cluster singles doubles and perturbative triples [CCSD(T)] method has emerged as the “gold-standard” method for describing weak intermolecular interactions such as hydrogen bonding. However, the high inherent computational expense and requirement for large basis sets, significantly limits the molecular size of complexes that can be studied with CCSD(T). The recently developed CCSD(T)-F12 methods, include explicit electron-electron correlation, which greatly increases the proportion of correlation energy obtained with a given basis set.^{24–26} The CCSD(T)-F12 methods have been shown to give very accurate intermolecular distances and interaction energies of hydrogen bonded complexes,²⁷ as well as accurate XH-stretching (X = O, C, F, Cl) fundamental and overtone transition wavenumbers and intensities.²⁸ For example, CCSD(T)-F12a interaction energies calculated with the VDZ-F12 basis set are found to be of equal accuracy to

^{a)} Author to whom correspondence should be addressed. Electronic mail: hgk@chem.ku.dk. Tel.: 45-353-20334. Fax: 45-353-20322.

results obtained with the much more computationally expensive CCSD(T)/aug-cc-pVQZ method.²⁷

In this work, we present the FTIR spectrum of the DMA-TMA complex in the NH-stretching fundamental region. To rationalize our experimental spectrum, we performed high level quantum chemical calculations with the CCSD(T)-F12a/VDZ-F12 method. We have also calculated the NH-stretching frequencies and oscillator strengths for DMA-TMA complex with an anharmonic oscillator local mode model.^{29,30} For comparison, calculations at the same level of theory were also completed for the DMA-DMA complex, which was recently measured.⁹

II. EXPERIMENTAL METHODS

The experimental setup has been described in detail elsewhere,⁹ therefore only a brief summary is given here. The DMA-TMA complex was studied with a Bruker Vertex 70 FTIR spectrometer using a 1.0 cm⁻¹ resolution. A CaF₂ beam splitter and an MCT (Mercury-Cadmium-Telluride) detector were fitted to the spectrometer. The FTIR spectrometer was purged with dry N₂ gas to minimize the interference by water vapor. The spectra were recorded at room temperature (298 K) using either a 10 cm path length gas cell equipped with KBr windows or for the low vapor pressure (2 Torr) reference spectrum of DMA, a 4.8 m path length gas cell (Infrared Analysis, Inc.) equipped with Infracil quartz windows. The gas samples were prepared with a glass vacuum line (J. Young) equipped with several pressure gauges.⁹ Known pressures of the two vapors were mixed for three days to ensure complete equilibrium. The pressure ranges used to obtain the spectra of the complex are 52–72 Torr and 264–367 Torr for DMA and TMA, respectively. In our experiments, vapor adsorption on the cell walls was very slow. The measured pressure uncertainty was smaller than 5% even after three days and was neglected. Spectral subtraction and analysis was performed with the OPUS and Origin software. DMA (anhydrous, 99+%) and TMA (anhydrous, 99%) were purchased from Aldrich and used without any further purification.

III. COMPUTATIONAL DETAILS

We have optimized the geometries of the DMA-TMA and DMA-DMA complexes and the constituent monomers with the B3LYP, LC-wPBE, M06-2X, and wB97XD functionals with the aug-cc-pVTZ basis set. Harmonic vibrational frequencies were also calculated to confirm that all the structures were true minima. All DFT calculations were performed with GAUSSIAN 09 using the “opt = vtight” and “int = ultrafine” options.³¹ We have also optimized the geometries of the complexes and monomers using the explicitly correlated CCSD(T)-F12a method with the VDZ-F12 basis set. The VDZ-F12 basis set is specifically optimized for use with explicitly correlated F12 methods and is of a similar size (but contain fewer diffuse basis functions) to the corresponding aug-cc-pVDZ basis set. All explicitly correlated calculations were performed with MOLPRO 2010.1 using the following optimization threshold criteria: gradient = 1 × 10⁻⁵ a.u., step

size = 1 × 10⁻⁵ a.u., and energy = 1 × 10⁻⁷ a.u., with all single point energies converged to 1 × 10⁻⁹ a.u.³² Density fitting approximations^{33,34} and the resolution of the identity (RI) approximation were utilized in the explicitly correlated calculations with the default auxiliary basis sets.^{35–37} The default CCSD-F12 correlation factor [(1/β)exp(-βr₁₂), where β = 1] was also used. In all calculations, only the valence electrons were correlated.

We have calculated the enthalpies and Gibbs free energies of formation for DMA-TMA and DMA-DMA at 298.15 K (ΔH_{298K}⁰ and ΔG_{298K}⁰) using standard statistical mechanics.

We calculate the NH-stretching wavenumbers and oscillator strengths for DMA-TMA and DMA-DMA with an anharmonic oscillator local mode model.^{29,30} This vibrational model has been previously shown to be appropriate for NH-stretching modes in a range of molecules.^{9,38–40} We assume that the NH-stretching vibrational mode can be described by a Morse oscillator, with the vibrational energy levels given by

$$\frac{E_v}{hc} = \left(v + \frac{1}{2}\right)\tilde{\omega} - \left(v + \frac{1}{2}\right)^2\tilde{\omega}x. \quad (1)$$

The Morse oscillator frequency ($\tilde{\omega}$) and anharmonicity ($\tilde{\omega}x$), are determined from the 2nd, 3rd, and 4th-order derivatives of the potential energy curve.³⁰ These derivatives are found by fitting a 12th-order polynomial to a 13-point CCSD(T)-F12a/VDZ-F12 calculated potential energy curve, obtained by displacing the NH bond from -0.30 to +0.30 Å in 0.05 Å steps around equilibrium.

The dimensionless oscillator strength f of a transition from the vibrational ground state $|0\rangle$ to a vibrationally excited state $|v\rangle$ is given by

$$f_{v0} = 4.702 \times 10^{-7} [\text{cm D}^{-2}] \tilde{\nu}_{v0} |\tilde{\mu}_{v0}|^2, \quad (2)$$

where $\tilde{\nu}_{v0}$ is the wavenumber of the vibrational transition in cm⁻¹ and $\tilde{\mu}_{v0} = \langle v | \tilde{\mu} | 0 \rangle$ is the transition dipole moment matrix in Debye (D). The transition dipole matrix element is expanded as

$$\langle v | \tilde{\mu} | 0 \rangle = \frac{1}{1!} \frac{\partial \tilde{\mu}}{\partial q} \langle v | q | 0 \rangle + \frac{1}{2!} \frac{\partial^2 \tilde{\mu}}{\partial q^2} \langle v | q^2 | 0 \rangle + \dots, \quad (3)$$

where q is the internal vibrational displacement coordinate. The dipole moment coefficients are found by fitting a 6th-order polynomial to a 15-point dipole moment function, obtained by displacing the NH bond from -0.30 to +0.40 Å in 0.05 Å steps around equilibrium and the expansion in Eq. (3) is limited to 6th-order.⁴¹

IV. RESULTS AND DISCUSSION

A. Calculated geometry and energy

In Fig. 1, we show the lowest energy structure of DMA-TMA (C_s symmetry) optimized with the CCSD(T)-F12a/VDZ-F12 method. Several other initial geometries were also attempted with the B3LYP and wB97XD methods, including rotating the DMA group about the internuclear axis and tilting its angle to the TMA group. However, these initial structures either converged to saddle points or to the

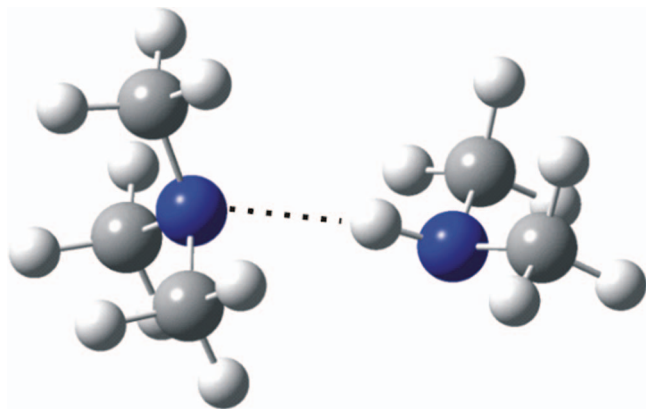


FIG. 1. Optimized structure of the DMA-TMA complex.

lowest energy structure. As expected, we find that the structure of DMA-TMA is similar to that of DMA-DMA, with a dominant $\text{NH}\cdots\text{N}$ hydrogen bonding interaction.⁹ In Table I, we present selected geometric parameters of the DMA-TMA and DMA-DMA complexes optimized with the CCSD(T)-F12a/VDZ-F12 method. We find that the NH bond length of the two complexes, and hence the elongation of the NH bond length upon complexation, is very similar. The $R(\text{NH}\cdots\text{N})$ intermolecular hydrogen bond distance of DMA-TMA is slightly (~ 0.01 Å) longer than the corresponding distance in DMA-DMA. The distance between the two N atoms [$R(\text{N}\cdots\text{N})$] in DMA-TMA is also 0.014 Å longer than that in DMA-DMA. The $\theta(\text{NH}\cdots\text{N})$ intermolecular hydrogen bond angles are found to be $\sim 27^\circ$ from the ideal linear orientation in both DMA-TMA and DMA-DMA, which suggests that both complexes exhibit weak hydrogen bonding interactions.¹⁵ As the key structural parameters for hydrogen bonding are similar in the two complexes, we expect that the hydrogen bonded NH-stretching spectral features of the two complexes will also be similar. Comparison with, for example, the $\text{OH}\cdots\text{O}$ bound water and methanol dimers, indicate that the angle of the hydrogen bond in the amine complexes deviates more from linearity than in the $\text{OH}\cdots\text{O}$ bound dimers and that the OO distance is shorter (less than 3 Å) than the NN distance (3.1 Å) found in the amine complexes.^{42,43}

In Tables II and III, we present the binding energies, zero point vibrational energy (ZPVE) corrected binding energies, enthalpies of formation ($\Delta H_{298\text{K}}^0$), and Gibbs free energies of formation ($\Delta G_{298\text{K}}^0$) for DMA-TMA and DMA-DMA. We have not corrected the CCSD(T)-F12a/VDZ-F12 binding energies for basis set superposition error (BSSE) using the

popular counterpoise approach as recent studies have shown that this actually gives results in poorer agreement with the CCSD(T) complete basis set limit than non-counterpoise corrected binding energies.^{44,45} Furthermore for a given basis set, the magnitude of BSSE obtained with explicitly correlated CCSD(T)-F12 calculations has been shown to be significantly smaller than the magnitude of BSSE obtained with conventional CCSD(T).^{44,45}

We find that the B3LYP/aug-cc-pVTZ and LC-wPBE/aug-cc-pVTZ binding energies are significantly underestimated as compared to the CCSD(T)-F12a/VDZ-F12 binding energy. These results are not surprising for the popular B3LYP functional, however better agreement was expected for the LC-wPBE functional.⁴⁶ In contrast, we find that the M06-2X/aug-cc-pVTZ and wB97XD/aug-cc-pVTZ results are in good agreement with the CCSD(T)-F12a/VDZ-F12 binding energies, with the former slightly underestimating and the later slightly overestimating the binding energies. The binding energy of the DMA-TMA complex is found to be slightly more negative (0.2 kJ mol⁻¹) than the binding energy of the DMA-DMA complex with the CCSD(T)-F12a/VDZ-F12 method. This result is corroborated only by the wB97XD binding energies, with the other three functionals all predicting that the DMA-DMA complex has a more negative binding energy than the DMA-TMA complex.

The enthalpy and Gibbs free energy of formation for a hydrogen bonded complex are very sensitive to the values of the calculated harmonic frequencies. This is particularly true for the low frequency intermolecular vibrational modes, which are generally highly anharmonic and dependent on the binding energy of the complex. These two characteristics may result in a fortuitous cancellation of errors, with an underestimated binding energy likely leading to underestimated harmonic frequencies that are then likely closer to the anharmonic fundamental transitions.

We find the enthalpies of formation for DMA-TMA and DMA-DMA are similar, differing by -0.1 to $+0.7$ kJ mol⁻¹ with the four functional used here. Slightly more variation is observed between the Gibbs free energies of formation for the two complexes with the DMA-TMA complex exhibiting less positive values than the DMA-DMA complex for a given functional ($+1.4$ to $+3.3$ kJ mol⁻¹). In Tables II and III we also present Gibbs free energies for DMA-TMA and DMA-DMA that include the CCSD(T)-F12a/VDZ-F12 binding energy and the thermal correction obtained with the different DFT methods. This binding energy correction significantly reduces the Gibbs free energy of formation obtained

TABLE I. Selected CCSD(T)-F12a/VDZ-F12 optimized geometric parameters of the DMA-TMA and (DMA)₂ complexes (in Å and degrees).

| Complex | $R(\text{NH}_b)$ | $\Delta R(\text{NH})^a$ | $R(\text{NH}_b\cdots\text{N})^b$ | $R(\text{N}\cdots\text{N})^c$ | $\theta(\text{NH}_b\cdots\text{N})^d$ | $\theta(\text{H}_b\cdots\text{NCC}_{\text{plane}})^e$ |
|---------|------------------|-------------------------|----------------------------------|-------------------------------|---------------------------------------|---|
| DMA-TMA | 1.0170 | 0.0049 | 2.1656 | 3.1102 | 153.7 | 96.5 |
| DMA-DMA | 1.0168 | 0.0048 | 2.1549 | 3.0961 | 153.1 | 98.9 |

^aChange in the bonded NH bond length upon complexation, i.e., $R(\text{NH}_b)_{\text{complex}} - R(\text{NH})_{\text{DMA}}$.

^bThe intermolecular hydrogen bond distance.

^cThe distance between the two N atoms.

^dThe intermolecular hydrogen bond angle.

^eThe angle between the donor hydrogen atom and the acceptor NCC plane.

TABLE II. Calculated binding energies (BE), zero point vibrational energy (ZPVE) corrected binding energies, enthalpies of formation (ΔH_{298K}^0), Gibbs free energies of formation (ΔG_{298K}^0) and equilibrium constant at 298 K (K_p) for DMA-TMA.^a

| | B3LYP/ aug-cc-pVTZ | LC-wPBE/ aug-cc-pVTZ | M06-2X/ aug-cc-pVTZ | wB97XD/ aug-cc-pVTZ | CCSD(T)-F12a/ VDZ-F12 |
|----------------------------------|-----------------------|-------------------------|------------------------|------------------------|--------------------------|
| BE | -9.8 | -11.3 | -21.0 | -23.2 | -22.0 |
| BE(ZPVE) | -6.9 | -8.2 | -17.3 | -19.5 | |
| ΔH_{298K}^0 | -4.1 | -5.6 | -15.2 | -17.1 | |
| ΔG_{298K}^0 | 21.8 | 23.3 | 17.5 | 12.9 | |
| ΔG_{298K}^0 ^b | 9.6 | 12.6 | 16.5 | 14.1 | |
| K_p | 1.5×10^{-4} | 8.4×10^{-5} | 8.5×10^{-4} | 5.5×10^{-3} | |
| K_p ^b | 2.1×10^{-2} | 6.2×10^{-3} | 1.3×10^{-3} | 3.5×10^{-3} | |

^aAll energies given in kJ mol^{-1} .

^bCalculated with the CCSD(T)-F12a/VDZ-F12 optimized electronic energies and the DFT thermal correction.

with the B3LYP and LC-wPBE functionals, with more modest changes in the M06-2X and wB97XD results. Overall, the similarity in the calculated binding energies, enthalpies and Gibbs free energies of formation for DMA-TMA and DMA-DMA suggests that the hydrogen bonded NH-stretching spectral features of the two complexes will also be similar.

It should be noted that the values of ΔH_{298K}^0 and ΔG_{298K}^0 for DMA-DMA calculated in our previous investigation with QCISD/aug-cc-pVTZ optimized electronic energies and B3LYP/aug-cc-pVTZ harmonic frequencies and rotational constants,⁹ differ significantly from those calculated with CCSD(T)-F12a/VDZ-F12 electronic energies and B3LYP/aug-cc-pVTZ thermal corrections (Table III). While the QCISD/aug-cc-pVTZ binding energy ($-21.1 \text{ kJ mol}^{-1}$) is similar to the CCSD(T)-F12a/VDZ-F12 binding energy ($-23.8 \text{ kJ mol}^{-1}$), the B3LYP values of the low frequency intermolecular vibrational modes are appreciably different in the two investigations, which significantly affects ΔH_{298K}^0 and ΔG_{298K}^0 . These differences are primarily attributed to the use of (in principle) less accurate numerical second derivatives in the previous investigation with MOLPRO and (in principle) more accurate analytical second derivatives in the present investigation with GAUSSIAN.

In summary, the CCSD(T)-F12 method is recommended for calculating the binding energies of complexes with the M06-2X and wB87XD DFT methods offering faster alternatives that seem to give accurate binding energies. Zero point vibrational energies (ZPVE) can be obtained from

B3LYP/aug-cc-pVTZ or other DFT calculations using the “opt = vtight” and “int = ultrafine” options, while the basis set superposition error (BSSE) correction is not necessary for the CCSD(T)-F12 binding energies. The thermal corrections can be obtained from the DFT calculations; however the variation between them is up to 8 kJ/mol for the two complexes investigated here. This certainly gives an indication of the sensitivity of thermal corrections to the level of theory.

B. Experimental NH-stretching spectra

In Fig. 2, we present the gas phase FTIR spectra of DMA, TMA and a mixture of the two gases. We subtract the individual monomer spectra from the spectrum of the mixture and attribute the residual absorption to the DMA-TMA complex (also shown in Fig. 2, lower trace). The sharp features in the residual DMA-TMA spectrum around 3600 cm^{-1} are attributed to H_2O impurities that are impossible to avoid due to the long mixing time.

The absorption spectrum of DMA-TMA has a peak at 3331 cm^{-1} with a full width at half maximum (FWHM) of 46 cm^{-1} . These values were obtained by fitting a Lorentzian function to the band. This band is assigned as the hydrogen bonded NH-stretching vibration of the DMA-TMA complex. In Table IV, we compare the experimental NH-stretching wavenumbers and FWHMs of DMA, DMA-TMA, and DMA-DMA. The NH-stretching transitions in the complexes are red shifted compared to the NH-stretching frequency in DMA.

TABLE III. Calculated binding energies (BE), zero point vibrational energy (ZPVE) corrected binding energies, enthalpies of formation (ΔH_{298K}^0), Gibbs free energies of formation (ΔG_{298K}^0) and equilibrium constant at 298 K (K_p) for DMA-DMA.^a

| | B3LYP/ aug-cc-pVTZ | LC-wPBE/ aug-cc-pVTZ | M06-2X/ aug-cc-pVTZ | wB97XD/ aug-cc-pVTZ | CCSD(T)-F12a/ VDZ-F12 |
|----------------------------------|-----------------------|-------------------------|------------------------|------------------------|--------------------------|
| BE | -10.6 | -11.8 | -21.3 | -22.8 | -21.8 |
| BE(ZPVE) | -7.5 | -8.3 | -16.9 | -18.6 | |
| ΔH_{298K}^0 | -4.8 | -6.0 | -15.3 | -16.7 | |
| ΔG_{298K}^0 | 23.2 | 25.4 | 20.8 | 16.1 | |
| ΔG_{298K}^0 ^b | 12.0 | 15.4 | 20.3 | 17.1 | |
| K_p | 8.7×10^{-5} | 3.5×10^{-5} | 2.3×10^{-4} | 1.5×10^{-3} | |
| K_p ^b | 7.9×10^{-3} | 2.0×10^{-3} | 2.8×10^{-4} | 1.0×10^{-3} | |

^aAll energies given in kJ mol^{-1} .

^bCalculated with the CCSD(T)-F12a/VDZ-F12 optimized electronic energies and the DFT thermal correction.

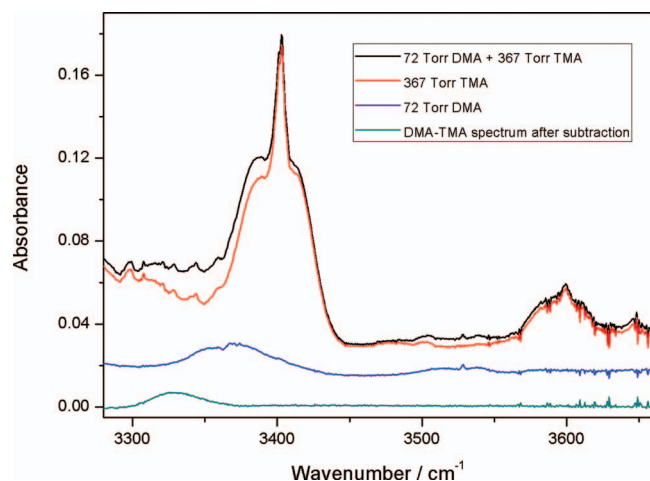


FIG. 2. Infrared spectra of DMA (blue), TMA (red) and a mixture of the two gases (black, top trace). The spectrum of the mixture after spectral subtraction of the monomer components is also shown in the figure (green, lower trace). The spectra were measured with a 10 cm path length cell at 298 K. For clarity, the three upper spectra are offset by 0.03, 0.03, and 0.01 absorbance units, respectively.

The red shift is 43 cm^{-1} in DMA-TMA, which is slightly larger than the 35 cm^{-1} red shift of DMA-DMA. This is perhaps expected as the additional CH_3 group in TMA donates additional electron density to the N atom, which is reflected in the slightly larger binding energy of the DMA-TMA complex with the CCSD(T)-F12a/VDZ-F12 method. The FWHM in the two complexes are quite similar, and significantly smaller than the FWHM of DMA. This is partly due to the tunneling splitting in DMA of $\sim 15\text{ cm}^{-1}$, which increases the overall (or apparent) width of its fundamental transition. The hydrogen bonding in the complex prevents the motion of the H-N-(CH_3)₂ umbrella motion and thereby the tunneling splitting.

The NH-stretching vibration of the DMA-TMA complex is difficult to observe because both DMA, TMA and for higher DMA pressures also the DMA-DMA complex have significant absorption between 3300 and 3400 cm^{-1} . To check the reproducibility of our experiment and to confirm the presence of a 1:1 binary complex, the spectra of the individual components and the mixtures were recorded at three different combinations of pressures. The resultant bands obtained from spectral subtraction in the three experiments have similar band shape and are shown in Fig. 3.

The chemical equilibrium for formation of the DMA-TMA complex can be written as



$$K_p = \frac{p_{\text{DMA-TMA}}}{p_{\text{DMA}} p_{\text{TMA}}}, \quad (5)$$

TABLE IV. Observed fundamental NH-stretching wavenumbers and bandwidths (in cm^{-1}).

| DMA ^a | | DMA-DMA ^b | | DMA-TMA | |
|------------------|------|----------------------|------|-------------|------|
| $\bar{\nu}$ | FWHM | $\bar{\nu}$ | FWHM | $\bar{\nu}$ | FWHM |
| 3374 | 57 | 3339 | 40 | 3331 | 46 |

^aFrom Ref. 38.

^bFrom Ref. 9.

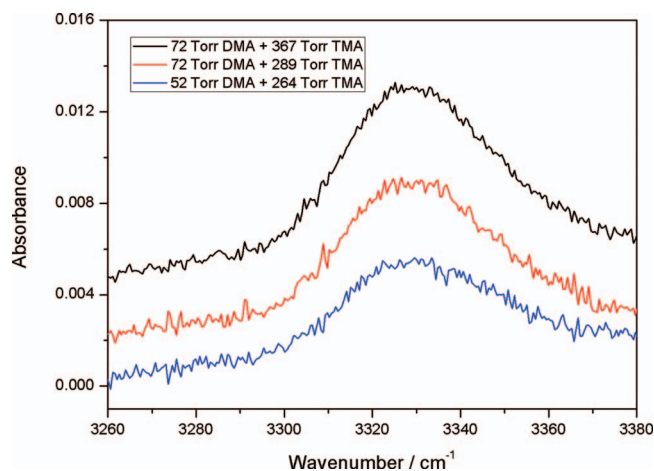


FIG. 3. The NH-stretching transition of DMA-TMA complex recorded with three different combinations of pressures. The spectra were measured with a 10 cm path length cell at 298 K. For clarity, the two upper spectra are offset by 0.004 and 0.002 absorbance units, respectively.

where K_p is the equilibrium constant and p_{DMA} , p_{TMA} , and $p_{\text{DMA-TMA}}$ are the vapor pressures of DMA, TMA, and the DMA-TMA complex, respectively. As shown in Fig. 4, the integrated intensity of the NH-stretching band in the three spectra (obtained from the three different pressure combinations) is found to be directly proportional to the product of the pressures of the two components, which indicates formation of a 1:1 complex.

In all experiments, we have restricted the pressure of DMA to less than ~ 70 Torr, to minimize formation of the DMA-DMA complex, which also absorbs strongly in the NH-stretching spectral region at 3339 cm^{-1} .⁹ In Fig. 5, we compare the absorption spectrum of the DMA-DMA complex (with a DMA pressure of 70 Torr) to the absorption spectrum of the DMA-TMA complex (with a mixture of 72 Torr DMA and 289 Torr TMA). The contours of the two bands in Fig. 5 are quite different, and even if the subtraction of the DMA spectrum was not perfect, the influence of the DMA dimer absorbance would be minimal. Again, the sharp features at around 3400 cm^{-1} and 3420 cm^{-1} in the DMA-TMA

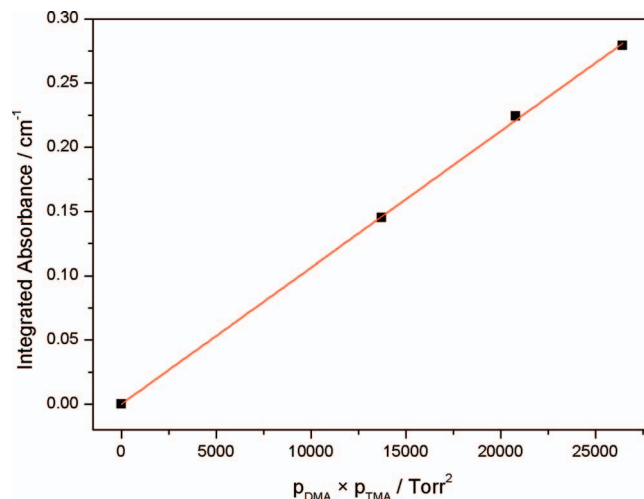


FIG. 4. The integrated absorbance of the NH-stretching band in DMA-TMA as a function of the product of the DMA and TMA pressures.

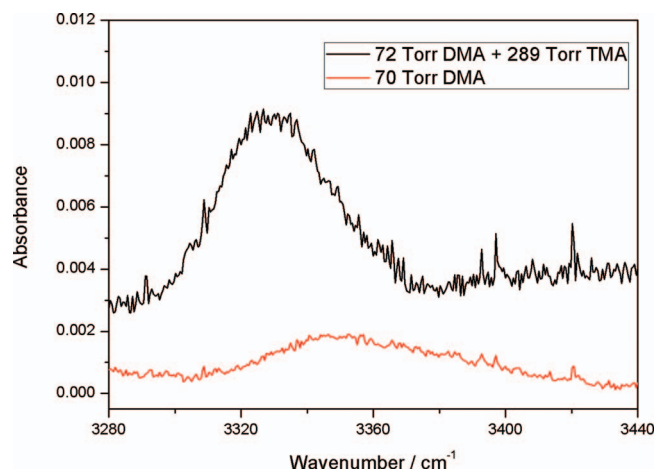


FIG. 5. Comparison of the NH-stretching spectra of DMA-TMA and $(\text{DMA})_2$. Both spectra are obtained after spectral subtraction of corresponding room temperature spectra of the monomers. For clarity, the DMA-TMA spectrum is offset by 0.002 absorbance units.

spectrum are due to water lines in this region, which are difficult to subtract completely.

C. Calculated NH-stretching transitions

We have used an anharmonic oscillator local mode model to calculate NH-stretching transitions in DMA, DMA-TMA, and DMA-DMA.^{29,30} In Table V, we present the calculated NH-stretching local mode parameters of DMA, DMA-TMA, and DMA-DMA obtained with the CCSD(T)-F12a/VDZ-F12 method. The calculated local mode parameters for DMA are close to the experimentally observed values of 3529.1 cm^{-1} and 77.7 cm^{-1} .³⁸ We find that the local mode frequencies ($\tilde{\omega}$) of the hydrogen bonded NH-stretching modes in DMA-TMA and DMA-DMA are $\sim 80 \text{ cm}^{-1}$ lower than that of DMA monomer whereas the local mode anharmonicities ($\tilde{\omega}x$) are $\sim 7 \text{ cm}^{-1}$ higher. This change in the local mode parameters upon complexation is typical of hydrogen bonded vibrational modes.^{11,14,47} The increase in $\tilde{\omega}x$ is also expected to increase the intensity of the fundamental NH-stretching transitions.⁴⁷

In Table VI, we present the CCSD(T)-F12a/VDZ-F12 calculated NH-stretching wavenumbers and intensities of DMA, DMA-TMA, and DMA-DMA obtained with our local mode model. For DMA monomer, we find that the calculated NH-stretching wavenumbers are slightly higher than, but nevertheless in good agreement with, experiment.³⁸ In the fundamental, first and second overtone regions, these differences are 8, 19, and 27 cm^{-1} , respectively. The CCSD(T)-F12a/VDZ-F12 calculated fundamental intensity is about half

TABLE V. Calculated NH-stretching local mode parameters (in cm^{-1}) of DMA, DMA-TMA, and $(\text{DMA})_2$ with the CCSD(T)-F12a/VDZ-F12 method.

| Parameter | DMA | DMA-DMA | | DMA-TMA |
|-------------------|---------|-----------------|-----------------|-----------------|
| | NH | NH _b | NH _f | NH _b |
| $\tilde{\omega}$ | 3536.28 | 3459.83 | 3535.72 | 3456.44 |
| $\tilde{\omega}x$ | 77.12 | 83.71 | 76.89 | 84.22 |

that measured,³⁸ whereas for the overtones the agreement is much better. Previous calculations with the CCSD(T)/aug-cc-pVTZ method gave a fundamental intensity that is within 10% of the experimental value.³⁸ The NH-stretching dipole moment function of DMA monomer is very flat at the equilibrium geometry, which leads to an anomalously low fundamental intensity that is difficult to calculate accurately.³⁸ Previous investigations have shown that XH-stretching intensities obtained with the CCSD(T)-F12a/VDZ-F12 method are close to those obtained at the CCSD(T)/CBS limit.²⁸

The calculated red shifts $\Delta\tilde{\nu}$ of the fundamental NH-stretching transitions of DMA-TMA and DMA-DMA are 94 cm^{-1} and 90 cm^{-1} , respectively. These calculated red shifts are significantly larger than the experimental red shifts of 43 cm^{-1} and 35 cm^{-1} . Some of this discrepancy between theory and experiment is likely due to the population of low frequency intermolecular vibrational modes in the room temperature experiments. This thermal excitation weakens the hydrogen bond, and therefore the frequency shift induced by hydrogen bonding appears less pronounced.¹³ For the $\text{CHCl}_3\text{-NH}_3$ complex, the bonded CH-stretching red shift at room temperature is approximately half (17.5 cm^{-1}) the magnitude of the corresponding red shift in a jet cooled expansion (38 cm^{-1}).^{12,13} The other major reason for the discrepancy is the neglect of vibrational coupling to the low-frequency intermolecular vibrational modes in the 1D AO model. In water dimer, comparison of a full 12D calculation with a model that ignores the intermolecular vibrations suggest that the OH_b-stretching transition frequency is increased by 26 cm^{-1} upon inclusion of the intermolecular coupling.^{48,49}

The intensity of the fundamental NH-stretching transition for the DMA-TMA complex is calculated to be approximately 700 times stronger than that for DMA monomer whereas for the DMA-DMA complex the equivalent transition is approximately 600 times stronger. This large intensity enhancement is due in part to the usual intensity enhancement of 10–50 times found in other hydrogen bond systems,^{11,14,50} which is exaggerated by the very weak intensity of the NH-stretching fundamental transition in DMA.³⁸ The weak fundamental in DMA is due to a very small first derivative of the dipole moment functions which changes significantly upon complex formation. This intensity increase for the fundamental transition is considered to be a criterion for hydrogen bonding.^{15,16} Indeed, it is because of the large intensity enhancement of the NH-stretching transition that we can observe these two complexes in the gas phase at room temperature despite their low equilibrium constants and the relatively small frequency shifts. Comparison of the experimentally integrated band intensity and the CCSD(T)-F12a/VDZ-F12 calculated oscillator strength of the NH-stretching band indicate that there is only about 0.04 Torr DMA-TMA complex present in a mixture of 72 Torr DMA and 367 Torr TMA at room temperature. As seen in Table VI, the intensities of NH-stretching overtone transitions ($\Delta\nu_{\text{NH}} = 2\text{--}5$) in DMA-TMA and DMA-DMA are quite small compared with the fundamental transitions. After taking into account the amount of complexes in the gas cells, we conclude that it is not possible to observe the overtone transitions of DMA-TMA or DMA-DMA with our experimental setup.

TABLE VI. Calculated NH-stretching wavenumbers (in cm^{-1}) and oscillator strengths for DMA, DMA-TMA, and $(\text{DMA})_2$.^a

| $\Delta\tilde{\nu}_{\text{NH}}$ | DMA | | $(\text{DMA})_2$ ^b | | | | DMA-TMA | | | |
|---------------------------------|-------|-----------------------|-------------------------------|---------------------|-----------------------|------------------------------|---------|---------------------|-----------------------|------------------------------|
| | ν | f_{D} | ν | $\Delta\tilde{\nu}$ | f_{DD} | $f_{\text{DD}}/f_{\text{D}}$ | ν | $\Delta\tilde{\nu}$ | f_{DT} | $f_{\text{DT}}/f_{\text{D}}$ |
| 1 | 3382 | 5.4×10^{-8} | 3292 | 90 | 3.3×10^{-5} | 611 | 3288 | 94 | 3.8×10^{-5} | 704 |
| 2 | 6610 | 3.7×10^{-7} | 6417 | 193 | 5.4×10^{-9} | 0.015 | 6408 | 202 | 8.7×10^{-9} | 0.024 |
| 3 | 9683 | 2.1×10^{-8} | 9375 | 308 | 3.8×10^{-9} | 0.18 | 9359 | 324 | 3.3×10^{-9} | 0.16 |
| 4 | 12603 | 1.1×10^{-9} | 12165 | 438 | 1.3×10^{-9} | 1.2 | 12141 | 462 | 1.3×10^{-9} | 1.2 |
| 5 | 15368 | 7.7×10^{-11} | 14788 | 580 | 1.7×10^{-10} | 2.2 | 14756 | 612 | 1.8×10^{-10} | 2.3 |

^aCalculated with the anharmonic oscillator local mode model with CCSD(T)-F12a/VDZ-F12 calculated parameters.^bResults are for the hydrogen bonded NH-stretching transition, NH_b .

D. Thermodynamic equilibrium constant

Based on Eq. (5), we can determine the thermodynamic equilibrium constant K_p at a certain temperature. This method has been previously used to determine K_p for other complexes.^{9,10,12} We estimate the partial pressure of the complex $p_{\text{DMA-TMA}}$ based on the measured intensity of the fundamental NH_b -stretching band and the calculated oscillator strength of this transition, which with the CCSD(T)-F12a/VDZ-F12 method is 3.8×10^{-5} . The oscillator strength of a transition is proportional to the integrated band area. At room temperature, 298 K, this relation can be written as^{40,51}

$$f = 8.026 \times 10^{-7} \text{ Torr m cm} \frac{1}{pl} \int A(\tilde{\nu}) d\tilde{\nu}, \quad (6)$$

where p is the pressure (in Torr), l is the path length (in meters), and the integrated absorbance is in cm^{-1} . In the present experiments on the DMA-TMA complex $l = 0.1$ m was used, and Eq. (6) can be rearranged to determine the pressure of the DMA-TMA complex

$$p_{\text{DMA-TMA}} = 8.026 \times 10^{-6} \text{ Torr cm} \frac{\int A(\tilde{\nu}) d\tilde{\nu}}{f_{\text{calc}}}. \quad (7)$$

A plot of $p_{\text{DMA-TMA}}$ determined from Eq. (7), against $p_{\text{DMA}} \times p_{\text{TMA}}$ for each of our three experiments is shown in Fig. 6.

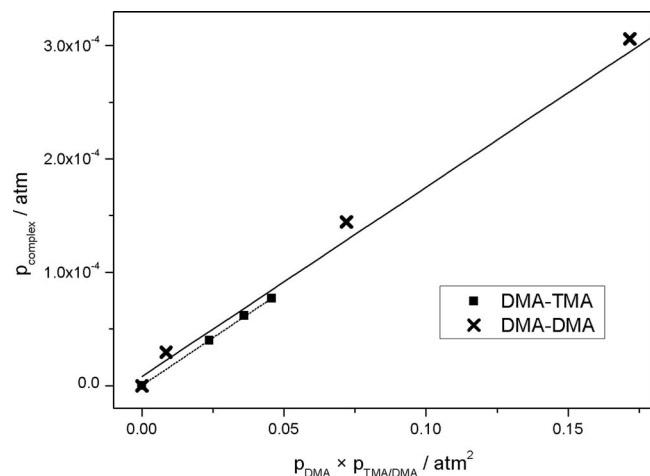


FIG. 6. The calculated $p_{\text{DMA-TMA}}$ (filled squares) against $p_{\text{DMA}} \times p_{\text{TMA}}$ and for comparison a few measurements of $p_{\text{DMA-DMA}}$ (crosses) against $p_{\text{DMA}} \times p_{\text{DMA}}$ from previous work.⁹ The partial pressure of the complex is estimated from the measured integrated of the fundamental NH_b -stretching band divided by the calculated oscillator strength of this transition as given in Table VI.

For comparison we also plot the equivalent results for DMA-DMA.⁹ The slope of the least-square fitting of these data is K_p . It is clear from the slope of the fitted lines in Fig. 6 that the two complexes have very similar K_p values, which is also in agreement with our calculated values. We determine K_p to be $1.7 \times 10^{-3} \text{ atm}^{-1}$ at room temperature of 298 K for both complexes. This value for DMA-DMA is slightly larger than the previously determined thermodynamic equilibrium constant of DMA dimer ($1.4 \times 10^{-3} \text{ atm}^{-1}$).⁹ In the previous paper, the K_p value was determined based on the ratio of fundamental NH-stretching intensity in DMA and DMA-DMA (details in Ref. 9 and its supporting information). However, due to the previously mentioned difficulty in accurately calculating the fundamental intensity of DMA monomer that does not occur in the complexes, we believe the present method is more reliable. We estimate the error in our calculated oscillator strength of the NH-stretching fundamental to be within a factor of 2.^{28,49} Therefore, we believe that the uncertainty of our determined K_p values is less than a factor of 3 when CCSD(T)-F12a/VDZ-F12 calculated oscillator strengths are used. This is significantly less than the variation in *ab initio* calculated K_p values.

We have also estimated the thermodynamic equilibrium constant K_p for DMA-TMA and DMA-DMA using the calculated Gibbs free energies in Tables II and III. Not surprisingly, we find that this value is very sensitive to the theoretical approach used. For DMA-TMA, our theoretical estimates of K_p range from 8.4×10^{-5} to $2.1 \times 10^{-2} \text{ atm}^{-1}$ whereas for DMA-DMA they range from 8.7×10^{-5} to $2.0 \times 10^{-3} \text{ atm}^{-1}$. These ranges reduce to within a factor of 30 when the more reliable CCSD(T)-F12/VDZ-F12 binding energies are used. The experimentally determined values of K_p for DMA-TMA and DMA-DMA both fit within the upper limits of these theoretical estimates. The wide variation in the calculated values of K_p again highlights the difficulty in accurately determining Gibbs free energies of formation for hydrogen bonded complexes.

V. CONCLUSIONS

The gas phase complex formed between dimethylamine and trimethylamine has been observed with FTIR spectroscopy and has been compared to previous results for the dimethylamine dimer. Comparable red shifts of the NH-stretching transition of the NH bond involved in hydrogen bonding were found in these two complexes. The intensity

enhancement of this band upon complexation is very large, approximately a factor of 700 and 600 in the DMA-TMA and DMA-DMA complexes, respectively. The similarity of the DMA-TMA and DMA-DMA complexes in the calculated binding energies and enthalpies of formation supports the similarity of the hydrogen bonded NH-stretching spectral features in these two complexes. The thermodynamic equilibrium constant K_p of DMA-TMA complexation at 298 K was determined based on the measured and calculated fundamental NH-stretching transition intensity and found to be very similar for the two complexes.

ACKNOWLEDGMENTS

We thank The Danish Council for Independent Research-Natural Sciences and the Danish Center for Scientific Computing (DCSC) for funding. We thank the University of Waikato High Performance Computing Facility for computer time.

- ¹A. A. Vigin, in *Molecular Complexes in Earth's Planetary, Cometary and Interstellar Atmospheres.*, edited by A. A. Vigin and Z. Slanina (World Scientific, River Edge, NJ, 1998), pp. 60–99.
- ²V. Vaida and J. E. Headrick, *J. Phys. Chem. A* **104**, 5401–5412 (2000).
- ³V. Vaida, H. G. Kjaergaard, and K. J. Feierabend, *Int. Rev. Phys. Chem.* **22**, 203–219 (2003).
- ⁴W. Klemperer and V. Vaida, *Proc. Natl. Acad. Sci. U.S.A.* **103**(28), 10584–10588 (2006).
- ⁵I. V. Ptashnik, K. M. Smith, K. P. Shine, and D. A. Newnham, *Q. J. R. Meteorol. Soc.* **130**(602), 2391–2408 (2004).
- ⁶D. J. Paynter, I. V. Ptashnik, K. P. Shine, and K. M. Smith, *Geophys. Res. Lett.* **34**(12), L12808, doi:10.1029/2007GL029259 (2007).
- ⁷V. Vaida, *J. Chem. Phys.* **135**(2), 020901 (2011).
- ⁸H. G. Kjaergaard, T. W. Robinson, D. L. Howard, J. S. Daniel, J. E. Headrick, and V. Vaida, *J. Phys. Chem. A* **107**(49), 10680–10686 (2003).
- ⁹L. Du and H. G. Kjaergaard, *J. Phys. Chem. A* **115**, 12097–12104 (2011).
- ¹⁰S. Chung and M. Hippler, *J. Chem. Phys.* **124**(21), 214316 (2006).
- ¹¹D. L. Howard and H. G. Kjaergaard, *Phys. Chem. Chem. Phys.* **10**(28), 4113–4118 (2008).
- ¹²M. Hippler, *J. Chem. Phys.* **127**(8), 084306 (2007).
- ¹³M. Hippler, S. Hesse, and M. A. Suhm, *Phys. Chem. Chem. Phys.* **12**(41), 13555–13565 (2010).
- ¹⁴D. L. Howard and H. G. Kjaergaard, *J. Phys. Chem. A* **110**(31), 9597–9601 (2006).
- ¹⁵E. Arunan, G. R. Desiraju, R. A. Klein, J. Sadlej, S. Scheiner, I. Alkorta, D. C. Clary, R. H. Crabtree, J. J. Dannenberg, P. Hobza, H. G. Kjaergaard, A. C. Legon, B. Mennucci, and D. J. Nesbitt, *Pure Appl. Chem.* **83**, 1619–1637 (2011).
- ¹⁶E. Arunan, G. R. Desiraju, R. A. Klein, J. Sadlej, S. Scheiner, I. Alkorta, D. C. Clary, R. H. Crabtree, J. J. Dannenberg, P. Hobza, H. G. Kjaergaard, A. C. Legon, B. Mennucci, and D. J. Nesbitt, *Pure Appl. Chem.* **83**, 1637–1641 (2011).
- ¹⁷J. D. Lambert and E. D. T. Strong, *Proc. R. Soc. London, Ser. A* **200**(1063), 566–572 (1950).
- ¹⁸T. Pradeep, M. S. Hegde, and C. N. R. Rao, *J. Mol. Spectrosc.* **150**(1), 289–292 (1991).
- ¹⁹J. A. Odutola, R. Viswanathan, and T. R. Dyke, *J. Am. Chem. Soc.* **101**(17), 4787–4792 (1979).
- ²⁰M. J. Tubergen and R. L. Kuczkowski, *J. Chem. Phys.* **100**(5), 3377–3383 (1994).
- ²¹R. B. Bohn and L. Andrews, *J. Phys. Chem.* **95**(24), 9707–9712 (1991).
- ²²U. Buck, X. J. Gu, R. Krohne, C. Lauenstein, H. Linnartz, and A. Rudolph, *J. Chem. Phys.* **94**(1), 23–29 (1991).
- ²³C. A. Hunter, *Angew. Chem., Int. Ed.* **43**(40), 5310–5324 (2004).
- ²⁴D. P. Tew, W. Klopper, C. Neiss, and C. Hattig, *Phys. Chem. Chem. Phys.* **9**(16), 1921–1930 (2007).
- ²⁵O. Marchetti and H. J. Werner, *Phys. Chem. Chem. Phys.* **10**(23), 3400–3409 (2008).
- ²⁶T. B. Adler, G. Knizia, and H. J. Werner, *J. Chem. Phys.* **127**(22), 221106 (2007).
- ²⁷J. R. Lane and H. G. Kjaergaard, *J. Chem. Phys.* **131**(3), 034307 (2009).
- ²⁸J. R. Lane and H. G. Kjaergaard, *J. Chem. Phys.* **132**(17), 174304 (2010).
- ²⁹B. R. Henry and H. G. Kjaergaard, *Can. J. Chem.* **80**(12), 1635–1642 (2002).
- ³⁰D. L. Howard, P. Jorgensen, and H. G. Kjaergaard, *J. Am. Chem. Soc.* **127**(48), 17096–17103 (2005).
- ³¹M. J. Frisch, G. W. Trucks, H. B. Schlegel *et al.*, GAUSSIAN 09, Revision A.02, Gaussian, Inc., Wallingford, CT, 2010.
- ³²H.-J. Werner, P. J. Knowles, F. R. Manby, M. Schütz *et al.*, MOLPRO, version 2010.1, a package of *ab initio* programs, 2011, see <http://www.molpro.net>.
- ³³F. R. Manby, *J. Chem. Phys.* **119**(9), 4607–4613 (2003).
- ³⁴H. J. Werner, T. B. Adler, and F. R. Manby, *J. Chem. Phys.* **126**(16), 164102 (2007).
- ³⁵F. Weigend, *Phys. Chem. Chem. Phys.* **4**(18), 4285–4291 (2002).
- ³⁶F. Weigend, A. Kohn, and C. Hattig, *J. Chem. Phys.* **116**(8), 3175–3183 (2002).
- ³⁷K. E. Yousaf and K. A. Peterson, *J. Chem. Phys.* **129**(18), 184108 (2008).
- ³⁸B. J. Miller, L. Du, T. J. Steel, A. J. Paul, A. H. Södergren, J. R. Lane, B. R. Henry, and H. G. Kjaergaard, *J. Phys. Chem. A* **116**, 290–296 (2012).
- ³⁹D. L. Howard, T. W. Robinson, A. E. Fraser, and H. G. Kjaergaard, *Phys. Chem. Chem. Phys.* **6**(4), 719–724 (2004).
- ⁴⁰B. I. Niefer, H. G. Kjaergaard, and B. R. Henry, *J. Chem. Phys.* **99**(8), 5682–5700 (1993).
- ⁴¹Z. Rong and H. G. Kjaergaard, *J. Phys. Chem. A* **106**, 6242–6253 (2002).
- ⁴²F. J. Lovas and H. Hartwig, *J. Mol. Spectrosc.* **185**(1), 98–109 (1997).
- ⁴³T. R. Dyke, K. M. Mack, and J. S. Muentzer, *J. Chem. Phys.* **66**(2), 498–510 (1977).
- ⁴⁴J. D. McMahon and J. R. Lane, *J. Chem. Phys.* **135**, 154309 (2011).
- ⁴⁵K. M. de Lange and J. R. Lane, *J. Chem. Phys.* **135**(6), 064304 (2011).
- ⁴⁶O. A. Vydrov and G. E. Scuseria, *J. Chem. Phys.* **125**(23), 234109 (2006).
- ⁴⁷G. R. Low and H. G. Kjaergaard, *J. Chem. Phys.* **110**(18), 9104–9115 (1999).
- ⁴⁸D. P. Schofield, J. R. Lane, and H. G. Kjaergaard, *J. Phys. Chem. A* **111**(4), 567–572 (2007).
- ⁴⁹H. G. Kjaergaard, A. L. Garden, G. M. Chaban, R. B. Gerber, D. A. Matthews, and J. F. Stanton, *J. Phys. Chem. A* **112**(18), 4324–4335 (2008).
- ⁵⁰D. L. Howard and H. G. Kjaergaard, *J. Phys. Chem. A* **110**(34), 10245–10250 (2006).
- ⁵¹P. W. Atkins and R. S. Friedman, *Molecular Quantum Mechanics*, 3rd ed. (Oxford University Press, Oxford, 1997).